tvst

Article

Effect of Physiological Oxygen on Primary Human Corneal Endothelial Cell Cultures

Sangita P. Patel[1–3], Brayan Calle Gonzalez[1,2], Nataliia Paone[4], Christian Mueller[4], Jamie C. Floss[4], Maria E. Sousa[1,2], and Michael Y. Shi[4]

[1] Ross Eye Institute, Department of Ophthalmology, Jacobs School of Medicine and Biomedical Sciences, State University of New York at Buffalo, Buffalo, New York, USA
[2] Research Service, Veterans Administration of Western New York Healthcare System, Buffalo, New York, USA
[3] Ophthalmology Service, Veterans Administration of Western New York Healthcare System, Buffalo, New York, USA
[4] Jacobs School of Medicine and Biomedical Sciences, State University of New York at Buffalo, Buffalo, New York, USA

Correspondence: Sangita P. Patel, Ross Eye Institute, 1176 Main St, Buffalo, NY 14209, USA. e-mail: sppatel@buffalo.edu

Received: September 23, 2021
Accepted: January 29, 2022
Published: February 22, 2022

Keywords: corneal endothelial cells; cell culture; Fuchs endothelial corneal dystrophy; oxidative damage

Citation: Patel SP, Calle Gonzalez B, Paone N, Mueller C, Floss JC, Sousa ME, Shi MY. Effect of physiological oxygen on primary human corneal endothelial cell cultures. Transl Vis Sci Technol. 2022;11(2):33, https://doi.org/10.1167/tvst.11.2.33

Purpose: Primary human corneal endothelial cells (HCEnCs) cultured in room air are exposed to significantly higher O_2 concentrations [O_2] than what is normally present in the eye. We evaluated the growth and metabolism of HCEnCs cultured under physiological [O_2] (2.5%; $[O_2]_{2.5}$) and room air ($[O_2]_A$).

Methods: Primary cultures of HCEnCs from normal donors and donors with Fuchs dystrophy were grown at $[O_2]_{2.5}$ and $[O_2]_A$. Growth and morphology were compared using phase-contrast microscopy, zonula occludens (ZO-1) localization, cell density measurements, and senescence marker staining. CD44 (cell quality) and HIF-1α (hypoxia-inducible factor-1α) levels were evaluated by Western blotting. Cell adaptability to a reversal of [O_2] growth conditions was measured with cell viability assays, and cell metabolism was assessed via oxygen consumption and extracellular acidification rates.

Results: HCEnCs grown at $[O_2]_A$ and $[O_2]_{2.5}$ displayed similar morphologies, ZO-1 localization, CD44 expression, and senescence. Cells from donors with Fuchs dystrophy grew better at $[O_2]_{2.5}$ than at $[O_2]_A$. HIF-1α was undetectable. Cells displayed greater viability at $[O_2]_{2.5}$ than at $[O_2]_A$. HCEnCs showed significantly greater proton leak ($P < 0.01$), nonmitochondrial oxygen consumption ($P < 0.01$), and spare capacity ($P < 0.05$) for oxygen consumption rates, and greater basal glycolysis ($P < 0.05$) with a decreased glycolytic reserve capacity ($P < 0.05$) for extracellular acidification rates.

Conclusions: Primary HCEnCs show unique metabolic characteristics at physiologic [O_2]. The effect of [O_2] for optimization of HCEnC culture conditions should be considered.

Translational Relevance: With the advance of cell-based therapeutics for corneal endothelial diseases, [O_2] should be considered an important variable in the optimization of HCEnC culture conditions.

Introduction

Corneal endothelial disease from conditions such as Fuchs endothelial corneal dystrophy (FECD) and pseudophakic bullous keratopathy is a leading cause for corneal blindness, accounting for more 30,000 corneal transplants in the United States annually.[1,2] Although corneal endothelial transplantation techniques have improved tremendously over the past two decades, new therapies involving ocular injections of cultured human corneal endothelial cells (HCEnCs) and tissue-engineered constructs with cultured HCEnCs are emerging.[3–5] The success of these new therapies entails the development of proper HCEnC culture conditions that maintain normal in vivo characteristics.

Cell-based therapeutics require the in vitro culture of HCEnCs from donor corneal tissue followed by cell expansion, and selection. In vivo, HCEnCs have limited proliferative capacity and accumulate markers of cell stress with age and disease.[6–12] With cell-based therapeutics, additional stress from suboptimal culture conditions could further limit the health and longevity of transplanted cells. This underscores the importance of optimizing the culture conditions for HCEnCs intended for transplantation to minimize the cell stress response.

HCEnC primary cultures for cell injection therapy and laboratory studies are cultured under room air with 5% CO_2 at 37°C in humidified cell culture incubators. However, mammalian cells in vivo are not exposed to the high levels of O_2 present in room air incubators (~18%).[13] Many cell types, particularly stem cells, demonstrate improved metabolism, increased proliferation, decreased senescence and enhanced differentiation when cultured at physiological O_2 (physioxic) conditions compared to those at ambient air.[14–16] In addition, O_2-dependent and O_2-regulated enzymes, organelles, and signaling pathways are affected by alterations in the O_2 concentration ($[O_2]$) of the cell culture.[17] Thus the culture of HCEnCs under routine laboratory culture conditions may be suboptimal for cell-based therapeutics.

The physioxic partial pressure of O_2 at the endothelial surface of the central human cornea is approximately 21 mm Hg (~2.8%).[18] This is substantially lower than the ~18% O_2 that is present in most ambient air tissue culture incubators. We hypothesized that the culture of primary HCEnCs at 2.5% O_2 ($[O_2]_{2.5}$), which more closely mimics the in vivo condition, would be more favorable to cell growth and metabolism than culture under ambient room air ($[O_2]_A$) conditions. In this descriptive study, we compared the growth and metabolism characteristics of normal and FECD-derived HCEnCs cultured at ambient and physiological $[O_2]$.

Methods

Corneal Tissue

This study was approved by the University at Buffalo and VA Western NY Healthcare System Institutional Review Boards and the VA Western NY Research and Development Committee and adhered to the tenets of the Declaration of Helsinki.

Whole human globes were obtained from the University at Buffalo Anatomical Gift Program within 24 hours of the death of the donors and used immediately to initiate experiments. Data available about the donors included age and cause of death. Diabetes status was not known. Corneoscleral buttons were dissected from the eyes and were examined for the presence of guttae. Corneas from the Anatomical Gift Program with guttae were not used in these experiments. Globes were examined for lens status.

Descemet's membrane samples from patients with FECD were obtained at the time of Descemet's stripping endothelial keratoplasty surgery. All patients provided written informed consent. Samples obtained at the time of surgery were immediately placed into 15 mL conical tubes containing 10 mL minimal medium (Human Endothelial Serum Free Medium, Gibco, Gaithersburg, MD, USA; 2% charcoal stripped fetal bovine serum; and 1× antibiotic/antimycotic; Supplementary Table S1) and were transported to the laboratory at room temperature.

Primary Culture of HCEnCs

Corneoscleral buttons were briefly rinsed with minimal medium. A Sinskey hook and jewelers' forceps were used to strip Descemet's membrane with the adherent endothelial cells taking care to avoid stromal fibers. The Descemet's membrane samples were placed into 15-mL conical tubes containing 10 mL minimal medium and incubated overnight at 37°C in a humidified 5% CO_2 tissue culture incubator.

The following day, tubes containing stripped membrane in minimal medium were centrifuged, and supernatant was aspirated. Pelleted stripped membranes were resuspended in 0.02% ethylenediamine tetra-acetic (E8008; Sigma-Aldrich, St. Louis, MO, USA) and incubated for one hour at 37°C. A flame-polished Pasteur pipette with a rubber bulb was used to agitate the sample to dissociate the HCEnCs. Cells were pelleted by centrifugation. The supernatant was removed, and the cell pellet was resuspended in growth medium (Opti-MEM1, Gibco; 8% fetal bovine serum; 200 mg/L $CaCl_2$; 0.08% chondroitin sulfate; 20 µg/mL ascorbic acid; 1× antibiotic/antimycotic; 100 µg/mL pituitary extract; 5 ng/mL epidermal growth factor; 50 µg/mL gentamicin; Supplementary Table S2). HCEnCs were distributed into culture plates coated with FNC coating mix (Athena Enzyme Systems, Baltimore, MD, USA). HCEnCs from each cornea were distributed equally between plates placed in either a 37°C, 5% CO_2 humidified incubator ($[O_2]_A$ environment), or an environmental chamber ($[O_2]_{2.5}$ environment; 2.5% O_2, 5% CO_2, balance N_2, humidified; Billups-Rothenberg, Inc., Del Mar, CA, USA). The $[O_2]$ during flushing of the environmental chamber was monitored with the GMS-5002 oxygen sensor (Billups-Rothenberg, Inc.). The stability of the low O_2 environment over time was verified with a co-incubated oxygen sensor probe (Wireless Oxygen Gas Sensor;

PASCO, Roseville, CA, USA). The GMS-5002 oxygen sensor was also used to note $[O_2]_A$ (18.7%). The size of the plates and number of wells were determined by the individual experimental protocols. For all experiments, HCEnC were expanded in growth medium for one to two weeks to confluence. HCEnCs were subsequently transitioned to stable mature phenotype by culturing in minimal medium (Supplementary Table S1) for an additional one to two weeks before experiments were performed (unless otherwise indicated).

Culture of FECD Corneal Endothelial Cells

Within six hours of surgery, the FECD specimen tube was placed in the $[O_2]_A$ tissue culture incubator overnight. After incubation, cells were cultured as detailed in "Primary Culture of HCEnCs." Cells were distributed equally into one well each in two 12-well plates (FNC-coated), with one plate incubated at $[O_2]_A$ and the other at $[O_2]_{2.5}$.

PC3 Cell Culture

PC3 cells were obtained from a colleague who had purchased them directly from ATCC (American Type Culture Collection, Manassas, VA, USA).[19] Cells were grown in RPMI 1640 medium (Invitrogen, Carlsbad, CA) with 10% fetal bovine serum and 1× antibiotic/antimycotic (Corning, Corning, NY, USA). Cells were maintained in a 5% CO_2, humidified, room air, 37°C incubator for propagation. For experimental protocols, cells between passages 11 to 13 (capillary immunoassays) and 26 to 34 (Western blots) were placed in $[O_2]_A$ and $[O_2]_{2.5}$ environments alongside HCEnC experiments.

Endothelial Cell Density (ECD) Measurements

ECD measurements were obtained from wells seeded with primary HCEnC at $[O_2]_A$ and $[O_2]_{2.5}$ for Seahorse XFe24 analyzer experiments as described below. Nuclei were stained with 4′,6-diamidino-2-phenylindole (DAPI) and digital fluorescence images acquired for cell count analysis (ImageJ; National Institutes of Health, Bethesda, MD) with conversion to ECD (cells/mm^2). Positive cell growth for each well (i.e., increase in cell number greater than the number of cells initially seeded) was considered ECD >50 cells/mm^2 and only wells with positive growth were included in analyses of ECD.

Statistical Analysis

The mean ECDs from each condition were compared with unpaired two-tailed Student's *t*-tests. Percentage of wells with growth under each analysis condition were compared with two-tailed Fisher exact tests. Results were considered significant at a $P < 0.05$.

Immunofluorescence Localization

Immunofluorescence localization was performed according to previous protocols.[20] Briefly, HCEnCs were grown on glass coverslips and cells were fixed for 10 minutes with 3% paraformaldehyde. Cells were rinsed three times with phosphate-buffered saline solution (PBS) and then permeabilized with 0.1% Triton X-100 for five minutes and washed two times with PBS. Cells were blocked by incubating for 30 minutes at room temperature with 10% goat serum (Invitrogen). Goat serum was then removed, and ZO-1 antibody conjugated to Alexa Fluor 488 was added (1:250; Invitrogen, catalog no. 339188), and the cells were placed on an orbital shaker for two hours at room temperature. Antibody solution was then removed, and cells were washed three times with PBS for five minutes with continuous gentle agitation on an orbital shaker. Coverslips containing cells were carefully placed cell-side down onto microscope slides containing a drop of Vectashield with DAPI (Vector Laboratories, Burlingame, CA, USA). Coverslips were sealed with nail polish and incubated at 4°C overnight. Samples were imaged by fluorescence microscopy with a Keyence scanner (Keyence BZ-X810; Keyence, Osaka, Japan) with identical exposure and acquisition settings.

ZO-1 Image Analysis

ZO-1 images were analyzed using FIJI (ImageJ, National Institutes of Health) using methods similar to those previously described by others.[21] Contrast and brightness of the images were adjusted to enhance endothelial cell borders and the green channel (ZO-1) was isolated. Binary conversion was performed using Minimum's thresholding (Image->Adjust->Auto Threshold). Manual noise removal was performed followed by binary operations of "dilation" and "erosion" to create a skeletonized matrix of endothelial borders. Cell count, individual cell size, and total area occupied by cells was calculated using "Particle Analyzer," excluding cells that bordered the edge of the region of interest. ECD was calculated by dividing cell count by the total area occupied by the cells. Coefficient of variation was calculated by dividing the standard deviation of cell size by the average cell size. Cells with six adjacent neighbors were identified using the "Neighbor Analysis" function of the BioVoxxel Toolbox plugin for FIJI (http://imagej.net/BioVoxxel_Toolbox; National Institutes of Health). The number of six-sided cells was divided by the total number of cells to return a hexagonality index.

β-galactosidase Stain

Dissociated primary HCEnCs were seeded into 12- or 24-well plates at $[O_2]_A$ and $[O_2]_{2.5}$, with cells from one donor cornea divided into one well per O_2 condition in 12-well plates and two wells per O_2 condition in 24-well plates. Cells were expanded and matured as described above. Cell senescence testing was performed using Senescence *β*-Galactosidase Staining Kit (9860S; Cell Signaling Technology, Danvers, MA, USA) according to the manufacturer's protocol. Briefly, minimal medium was aspirated from the wells. Cells were rinsed one time with PBS at 37°C followed by addition of 250 µL 1× dilution of manufacturer-supplied fixative solution. Cells were incubated with fixative solution for 15 minutes at room temperature followed by three washes with PBS. Cells were stained by adding 250 µL *β*-galactosidase staining solution and incubating overnight at 37°C in a nonhumidified room air incubator. Positive cells were counted manually by direct visualization using phase-contrast microscopy. The *β*-galactosidase staining solution was then removed, and DAPI solution was added. Digital images of the DAPI-stained nuclei were obtained (Keyence) and analyzed (similarly to ECD analysis) for total cell count determination.

Statistical Analysis

The percentage of positive cells under the $[O_2]_A$ and $[O_2]_{2.5}$ conditions were compared using unpaired, two-tailed Student's *t*-tests.

Cell Viability Assay

HCEnC cultures were initiated in 96-well plates, with cells from one cornea seeded into 14 wells divided between two plates, with one plate at $[O_2]_A$ and one at $[O_2]_{2.5}$ and two wells with medium only in each plate as negative controls. The cells were grown and matured as per the "Primary Culture of HCEnCs" protocol above. In the maturation phase, at predetermined time points, the cell culture plates were placed into the opposite $[O_2]$ culture conditions to assess the response of the cells to the altered O_2 conditions. Cell viability was measured with the RealTime-Glo Cell Viability Assay (Promega, Madison, WI, USA). Briefly, MT Cell Viability Substrate and NanoLuc Enzyme diluted 1:2000 in 100 µL culture medium was added to each well, including those serving as negative controls. Metabolically active cells produced quantifiable luminescent signal, which was measured with a Synergy HT plate reader (BioTek, Winooski, VT, USA). Because the assay is not a terminal assay and the substrate luminescence can be monitored for up to 72 hours, measurements were taken every 24 hours without any additional substrate addition for that time frame.

Statistical Analysis

Because of the large differences between data from cells at $[O_2]_A$ vs. $[O_2]_{2.5}$, raw data were normalized with $\log_2$ transformation, and means were compared using paired, two-tailed Student's *t*-tests with significance set at a P value <0.05.

Measurement of Oxidative and Glycolytic Metabolism

Mitochondrial respiration (O_2 consumption rate [OCR]) and glycolysis (extracellular acidification rate [ECAR]) were measured with the Seahorse XFe24 (Agilent Technologies, Inc., Santa Clara, CA, USA). Dissociated primary HCEnCs (as per the protocol above) were seeded directly into FNC-coated Seahorse XFe24 culture plates, with cells from one cornea seeded into 10 wells equally distributed in two plates, with one plate incubated at $[O_2]_A$ and one at $[O_2]_{2.5}$. Cells were expanded in growth medium and matured in minimal medium. The evening before the experiment, two Seahorse XFe24 sensor cartridges were hydrated by adding 1 mL Seahorse Calibration solution to each of the wells. Cartridges were placed back in their original packaging, which was taped shut, and incubated overnight in a non-CO_2 37°C incubator. Assay medium was prepared on the day of the experiment and consisted of Seahorse XF Dulbecco's modified Eagle medium (DMEM), with 1.2 mM glutamine, 7.0 mM glucose, and 0.45 mM pyruvate. These substrate concentrations were selected to be approximately double the aqueous humor concentrations but in similar ratios to each other.[22–24] Drug stock solutions were prepared as follows: 10 mM oligomycin in 100% ethanol (O4876, Sigma-Aldrich), 10 mM carbonyl cyanide 4-(trifluoromethoxy) phenylhydrazone in 100% ethanol (FCCP, C2920; Sigma-Aldrich), 10 mM rotenone in dimethyl sulfoxide (R8875; Sigma-Aldrich), 10 mM antimycin A in 100% ethanol (A8674; Sigma-Aldrich), 500 mM 2-deoxy-D-glucose (2-DG) in Seahorse XF DMEM (D8375, Sigma-Aldrich). Drugs, diluted in Seahorse XF DMEM, were loaded into ports of the calibration plate. Cells were washed with PBS warmed to 37°C and then filled with

450 μL assay medium. Cells were incubated for one hour in a non-CO_2 37°C incubator before loading the plate into the Seahorse XFe24 analyzer. OCR and ECAR measurements were performed at baseline (B) and after additions of oligomycin (O, 1 μM), FCCP (1.5 μM), rotenone/antimycin A (RA, 0.5 μM), and 2-DG (50 mM). We calculated basal respiration (B-RA for OCR and B-2DG for ECAR), adenosine triphosphate (ATP) linked respiration (B-O), proton leak (O-RA), max respiration (FCCP-RA), spare capacity (FCCP-B), non-mitochondrial O_2 consumption (RA), and glycolytic reserve capacity (O-B). After completing the assay, cells were stained with DAPI and imaged, and cell nuclei were counted to normalize OCR and ECAR to cell density.

Statistical Analysis

Mean values were compared between $[O_2]_A$ and $[O_2]_{2.5}$ conditions using unpaired two-tailed *t*-tests.

Protein Preparations

Confluent matured cultures were lysed on ice with buffer containing 50 mM Tris (pH 7.4), 250 mM NaCl, 2 mM ethylenediaminetetraacetic acid (pH 8.0), and 10% Protease Inhibitor Cocktail (Sigma-Aldrich), 10% Triton X-100. Lysed cells were scraped from the dish, incubated on ice for 60 minutes, and spun in a centrifuge to pellet cell debris. The supernatant was collected, and protein concentration was measured with the Pierce BCA kit (Thermo Fisher Scientific, Waltham, MA, USA).

Western Blot

Proteins were separated on Mini-PROTEAN TGX Precast Gels (Bio-Rad Laboratories, Hercules, CA, USA) and transferred to PVDF membranes. Membranes were blocked (10% goat serum for CD44 blot or 5% nonfat milk [Blotting-Grade Blocker, Bio-Rad] for HIF-1*α* blot) for one hour followed by incubation overnight at 4°C in primary antibodies (CD44 [E7K2Y] XP Rabbit monoclonal antibody, diluted 1:1000, Cell Signaling Technology, Danvers, MA, USA; HIF-1*α* [D1S7W] XP Rabbit monoclonal antibody diluted 1:1000, Cell Signaling Technology). Membranes were then washed in tris-buffered saline-Tween 20 (TBST) three times and incubated for one hour at room temperature in secondary antibody (Alkaline Phosphatase–conjugated Anti-Rabbit IgG [A9919]; Sigma-Aldrich) diluted at 1:3000. After three washes in TBST, ECF substrate (Cytiva Amersham, Marlborough, MA, USA) was applied, and the blot was imaged with a ChemiDoc MP Imaging System (Bio-Rad). Membranes were then incubated twice (first for 10 minutes then for five minutes) with stripping buffer (1.5% glycine, 0.1% SDS, 1% TWEEN 20, pH 2.2) followed by four washes with TBST. Membranes were blocked one hour in 10% goat serum, then incubated for two hours at 4°C with alpha-tubulin mouse monoclonal antibody (1:1500, DM1A; Cell Signaling Technology). The membrane was washed with TBST three times and was incubated for one hour at room temperature with alkaline phosphatase-conjugate anti-mouse IgG secondary antibody (1:3000; A4312; Sigma-Aldrich). After three washes in TBST, ECF substrate was applied, and the blot was again imaged. Bands were quantified and normalized to the alpha-tubulin signal using Image Lab software (version 6.0.1; Bio-Rad).

Capillary Immunoassay

Capillary immunoassay was performed using the Jess Simple Western system (ProteinSimple; Bio-Techne, San Jose, CA, USA) per manufacturer instructions. Protein samples were prepared at 0.3 μg/μL and separated using the 12–230 kDa separation module. HIF-1*α* antibody was used at 1:20 dilution, and *α*-tubulin antibody was used at 1:150 dilution. The anti-rabbit and anti-mouse chemiluminescent detection modules (ProteinSimple) were used with antibodies diluted 1:2. Data were analyzed with Compass for Simple Western (ProteinSimple).

Results

Growth and Cell Markers of HCEnCs at $[O_2]_A$ and $[O_2]_2$

HCEnCs grown at $[O_2]_A$ and $[O_2]_{2.5}$ were observed by phase-contrast microscopy and demonstrated no differences in morphology (Fig. 1A). We used ZO-1 immunolocalization to assess tight junction integrity and evaluate metrics of cell density, coefficient of variation, and hexagonality under both growth conditions (Fig. 1B). We found a range of values for these metrics that we attribute to the wide age range and decreased growth of cells from older donors (n = 4 corneas, donor ages 60–93 years). Data are thus presented for individual corneas. Overall, ECD values were consistently higher in cultures grown at $[O_2]_{2.5}$ compared to $[O_2]_A$. Metrics for coefficient of variation, a measure of variability in cell size, and percentage of hexagonal cells (6A) did not show consistent differences between the culture conditions.

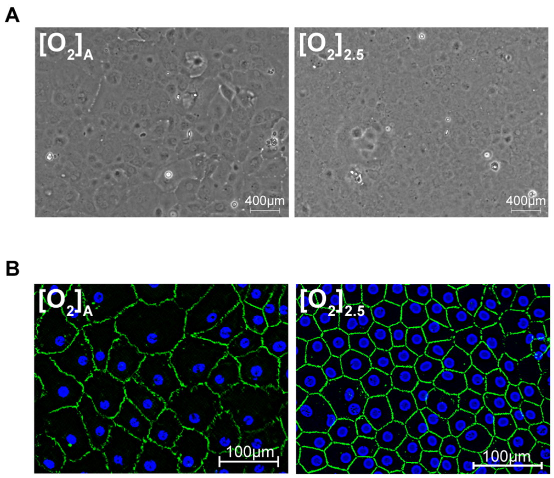

$[O_2]_A$				$[O_2]_{2.5}$		
ECD	COV	6A	age	ECD	COV	6A
389	0.37	37	**60**	872	0.39	67
108	0.31	45	**86**	230	0.36	31
134	0.50	27	**93**	263	0.38	35
116	0.63	30	**93**	151	0.21	29

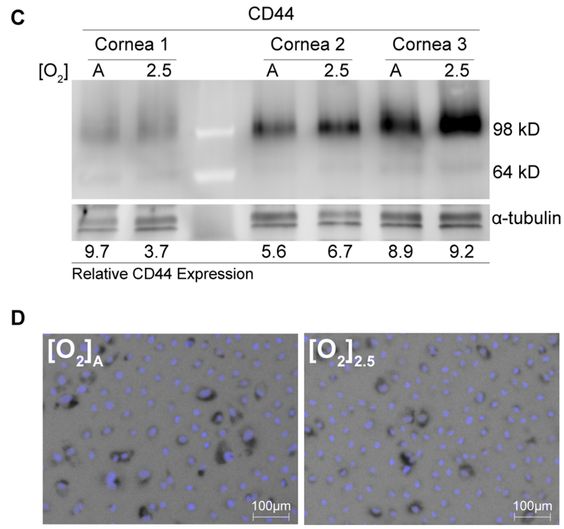

Figure 1. Human corneal endothelial cells cultured at $[O_2]_{2.5}$ demonstrate similar growth characteristics to cells grown at $[O_2]_A$. (A) Phase-contrast microscopy of HCEnC cultures shows similar cell morphology under both culture conditions. (B) Immunofluorescence imaging for zonula occludens (ZO-1, *green*) with DAPI-stained nuclei (*blue*) demonstrates similar integrity of tight junctions under both conditions (representative images from HCEnC cultures from n = 4 corneas). Quantification of cell characteristics for the data from four corneas. ECD, coefficient of variation (COV), and hexagonality (6A). (C) Western blot comparing CD44 expression in HCEnCs from three different donors grown at the different oxygen concentrations. CD44 expression levels were normalized to α-tubulin expression, showing the variability between donor corneas. (D) Senescence-associated β-galactosidase staining (*black*) with DAPI-stained nuclei (*blue)* shows similarities in percentage of senescent cells (mean ± SD: $[O_2]_A$ 58.3% ± 15.8%, and $[O_2]_{2.5}$ 53.8% ± 21.4%).

CD44 has been described as a marker for cell state in HCEnCs with $CD44^+$ status associated with cell state transition and $CD44^-$ associated with mature HCEnCs.[3,25] Cells selected for cell injection therapy for endothelial diseases are $CD44^-$.[3] We investigated whether CD44 expression was altered by the $[O_2]$ of the culture environment (Fig. 1C). Although there were differences in CD44 expression among HCEnC cultures from different donors, there was no consistent trend with regard to CD44 expression between $[O_2]_A$ and $[O_2]_{2.5}$ cultures (n = 4 corneal donors).

We next evaluated whether cell senescence was altered by the $[O_2]$ environment of the cells. β-Galactosidase staining was evaluated in HCEnC cultures from five donors. The percentages of β-galactosidase positive cells were high but did not differ significantly different between the $[O_2]$ culture conditions (mean ± SD: $[O_2]_A$ 58.3% ± 15.8%, and $[O_2]_{2.5}$ 53.8% ± 21.4%; $P = 0.711$; Fig. 1D). We attribute the high overall percentage of positive cells to the mean age of 81 years for these donor corneas.

HCEnC Growth by Donor Characteristics

The growth characteristics of HCEnCs under the two conditions were analyzed according to donor sex, lens status of the eye (phakic natural crystalline lens versus post cataract surgery with posterior chamber intraocular lens), and donor age group (Table 1). We hypothesized that cells with increased cumulative stress, for example, those from older donors or after cataract surgery, would have improved growth at $[O_2]_{2.5}$ compared to that at $[O_2]_A$ as a result of less oxidative stress from the lower, physiological $[O_2]$ environment. We did not find significant differences in HCEnC growth for any of these categories. We did note a trend toward improved growth at $[O_2]_{2.5}$ compared to that at $[O_2]_A$ for pseudophakic eyes; however, pseudophakic eyes were from significantly older donors than phakic eyes. There were no significant differences in ECDs among any of the categories. The low ECD noted in our cultures (mean donor age = 73 years) is consistent with previously published observations of lower ECD in older donors than in younger ones.[11]

Table 1. Growth Characteristics of HCEnCs at $[O_2]_A$ Versus $[O_2]_{2.5}$

Attributes	N	Wells With Growth (%) $[O_2]_A$	Wells With Growth (%) $[O_2]_{2.5}$	Wells With Growth (%) *P* Value	ECD ± SD (Cells/mm²) From Wells With Growth $[O_2]_A$	ECD ± SD (Cells/mm²) From Wells With Growth $[O_2]_{2.5}$	ECD ± SD *P* Value	Mean Age ± SD	*P* Value*
All Corneas	34	60%	72%	0.082	237 ± 127	209 ± 97	0.151		
Sex									0.001
Female	16	59%	72%	0.178	210 ± 95	222 ± 100	0.980	64.1 ± 13.6	
Male	18	61%	72%	0.378	269 ± 151	207 ± 93	0.056	80.1 ± 11.5	
Lens Status									<0.001
Phakic	16	76%	78%	0.829	258 ± 133	231 ± 99	0.239	63.8 ± 15.2	
pcIOL†	18	43%	63%	0.090	186 ± 91	182 ± 82	0.877	80.5 ± 10.1	
Age Group‡									<0.001
<72 years	17	77%	84%	0.370	257 ± 132	230 ± 91	0.608	61.3 ± 11.1	
≥72 years	17	38%	54%	0.143	180 ± 82	166 ± 88	0.240	83.8 ± 8.0	

**P* value comparing mean age.
†Posterior chamber intraocular lens.
‡Divided by median age of 72.

We further evaluated the effects of $[O_2]$ culture condition on HCEnCs cultured from patients with FECD. Because of the role of oxidative stress in FECD pathophysiology, we hypothesized that an $[O_2]$ closer to physiological conditions ($[O_2]_{2.5}$) would be more favorable for growth than $[O_2]_A$. The effects of $[O_2]$ on cell growth was readily apparent in cultures of FECD cells (Table 2). Fifty percent (6/12) of FECD HCEnC cultures grew better at $[O_2]_{2.5}$ than $[O_2]_A$.

Table 2. Growth at $[O_2]_A$ and $[O_2]_{2.5}$ of Primary Cultures of Corneal Endothelial Cells From Individuals With Severe FECD

Age (Years)	Sex	Lens Status	FECD Grade*	$[O_2]_A$	$[O_2]_{2.5}$
71	F	Phakic	6	−	−
68	F	Phakic	6	−	+
69	M	Phakic	5	−	+
79	F	pcIOL	5	−	++
70	F	Phakic	6	−	+++
77	F	pcIOL	6	+	++
67	M	Phakic	4	++†	+++
37	F	pcIOL	5	+++	+++
64	M	Phakic	6	+++	+++
67	M	Phakic	4	+++	+++
75	F	Phakic	6	+++	+++

pcIOL, pseudophakic posterior chamber intraocular lens.
*Modified Krachmer grade.[51]
†Cells demonstrated transformation from endothelial to fibroblast morphology.
− No cell proliferation.
+Minimal cell proliferation.
++Moderate cell proliferation, but not to confluence.
+++Cell proliferation to confluence.

Hypoxia-Inducible Factor-1*α* in HCEnC

Because of dramatic difference in $[O_2]$ between $[O_2]_A$ and $[O_2]_{2.5}$, we investigated whether our cells at $[O_2]_{2.5}$ were hypoxic by assaying for hypoxia-inducible factor-1α (HIF-1α) expression. We evaluated HIF-1α expression by Western blotting after incubating the cells at $[O_2]_A$ (n = 5 corneas), $[O_2]_{2.5}$ (n = 7 corneas), or at 0% O_2 (with 5% CO_2, balance N_2; eight-hour exposure; n = 2 corneas; Fig. 2A) with each set of hypoxia experiments performed on different days. For positive control, we co-incubated PC3 cell cultures with our HCEnC cultures. We harvested the cell lysates within minutes of opening the environmental chambers because of the rapid degradation of HIF-1α.[26] We did not detect HIF-1α expression in HCEnC at $[O_2]_{2.5}$ or at 0% O_2. By contrast, PC3 cells co-incubated with HCEnCs had increased HIF-1α expression at 0% O_2 compared with that at $[O_2]_A$. We also tried to chemically increase HIF-1α in HCEnCs by exposing the cells for 24 hours to 100 µM cobalt chloride. HIF-1α is degraded within minutes of exposure to normoxia through the action of prolyl hydroxylases. Cobalt chloride stabilizes HIF-1α expression through binding to prolyl hydroxylases, thus preventing HIF-1α degradation.[26] Cobalt chloride (100 µM) did not increase HIF-1α expression

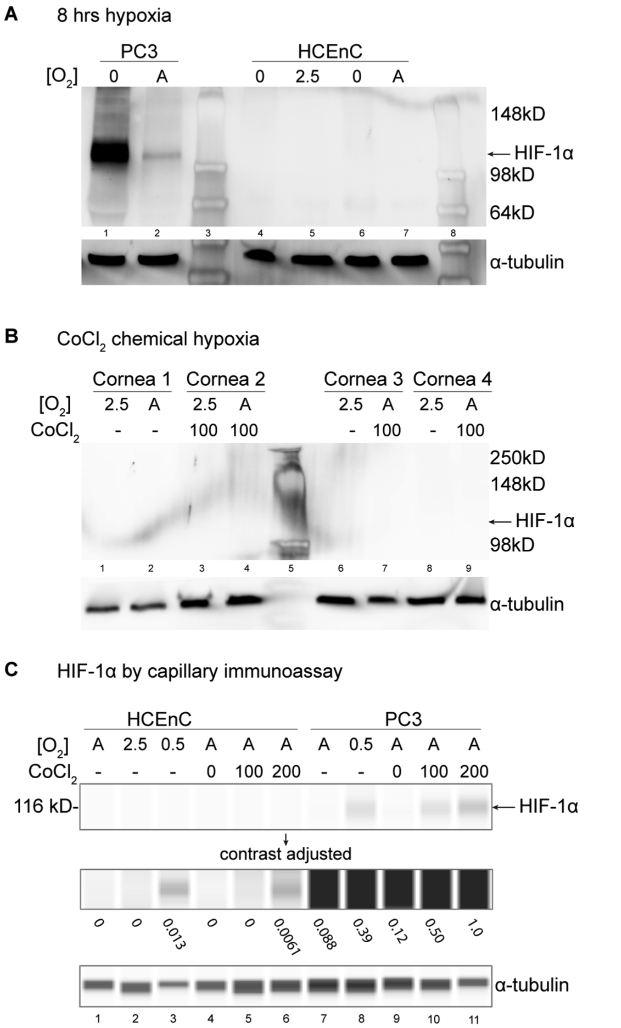

Figure 2. Cells grown at $[O_2]_{2.5}$ do not express HIF-1α. Western blots for HIF-1α. (A) PC3 cells (prostate cancer cell line, lanes 1, 2) were grown to confluence at $[O_2]_A$. HCEnC were expanded and matured at $[O_2]_{2.5}$ lanes (4, 5) and $[O_2]_A$ (lanes 6, 7). Cells of lanes 1, 4, and 6 were then simultaneously incubated in a 0% O_2 environment for eight hours. Ladder lanes 3, 8. 25 µg protein loaded per well. (B) HCEnCs expanded and matured at $[O_2]_{2.5}$ (lanes 1, 3, 6, 8) and $[O_2]_A$ (lanes 2, 4, 7, 9). Select cells were incubated for 24 hours with 100 µM cobalt chloride (lanes 3, 4, 7, and 9). 15 µg protein loaded per well. (C) Simple Western capillary immunoassay for HIF-1α. HCEnCs were expanded and matured at $[O_2]_{2.5}$ (lane 2) and $[O_2]_A$ (lanes 1, 3–6). PC3 cells were grown to confluence at $[O_2]_A$. Cells of lanes 3 and 8 were then simultaneously incubated in a 0.5% O_2 environment for four hours. Cells were incubated 24 hours at $[O_2]_A$ with 0 (lanes 4 and 9), 100 (lanes 5 and 10) or 200 (lanes 6 and 11) µM cobalt chloride. Contrast adjusted for HIF-1α signal to optimize view of the weak HIF-1α signal in HCEnCs in the image indicated. Signal intensities based on areas of the HIF-1α signal peaks normalized to tubulin and indicated below the band. HIF-1α signals with signal/noise ratios $<$10 are noted as 0.

in HCEnCs (n = 4 corneas; Fig. 2B). Because of the lack of a positive signal for HIF-1α in HCEnCs by Western blotting, we performed additional experiments (n = 4 corneas from two donors) with analysis by Jess Simple Western capillary immunoassay (Fig. 2C). For these experiments, in addition to HCEnC and PC3 cell co-incubations at $[O_2]_A$ and $[O_2]_{2.5}$, we evaluated 0.5% O_2 exposure for four hours (to alleviate concerns of toxicity and cell death to cells at the 0% O_2 condition) and also tested both 100 and 200 µM concentrations of cobalt chloride. We found robust expression of HIF-1α in PC3 cells at 0.5% O_2 and with 100 and 200 µM cobalt chloride. There was no HIF-1α expression in HCEnC at comparable levels to the PC3 cells. However, compared to PC3 cells, HCEnC at 0.5% O_2 (in one of two donors) or with 200 µM cobalt chloride (in both donors) showed a faint, positive signal for HIF-1α at approximately 100-fold lower level. Low levels of HIF-1α in normal compared to tumor cells has been noted before and may account for this large expression difference between PC3 cells and HCEnCs.[27] No signal was detected at $[O_2]_{2.5}$, thus confirming that the $[O_2]_{2.5}$ condition is not hypoxic for HCEnCs.

Viability of HCEnC at $[O_2]_A$ Versus $[O_2]_{2.5}$

We investigated the viability of HCEnC at $[O_2]_A$ and $[O_2]_{2.5}$ over time using a nonterminal viability assay (RealTime-Glo). This assay measures the reducing potential of cells as an indicator of cell viability. Measurements were performed at multiple time points including the growth phase, as well as measurements of the matured HCEnC monolayer (Fig. 3A). With this protocol, measurements were also performed on reversal of $[O_2]$ culture conditions to assess the ability of the cells to adapt. We found that cell viability was significantly higher for cells in the $[O_2]_{2.5}$ environment at each time point regardless of prior culture conditions, and the cells adapted rapidly to changes in $[O_2]$ environment (Fig. 3B). Under steady $[O_2]$ conditions, HCEnCs consistently showed significantly greater viability at $[O_2]_{2.5}$ than at $[O_2]_A$ (Fig. 3C).

Metabolism of HCEnC at $[O_2]_A$ Versus $[O_2]_{2.5}$

The reducing potential of a cell, as measured by the RealTime-Glo assay, is associated with cellular respiration and oxidative phosphorylation.[28, 29] To further understand the basis for the increased viability of HCEnC at $[O_2]_{2.5}$ versus that at $[O_2]_A$ as measured with the RealTime-Glo assay, we measured oxidative respiration and glycolysis under these conditions with the Seahorse Extracellular Flux Analyzer.

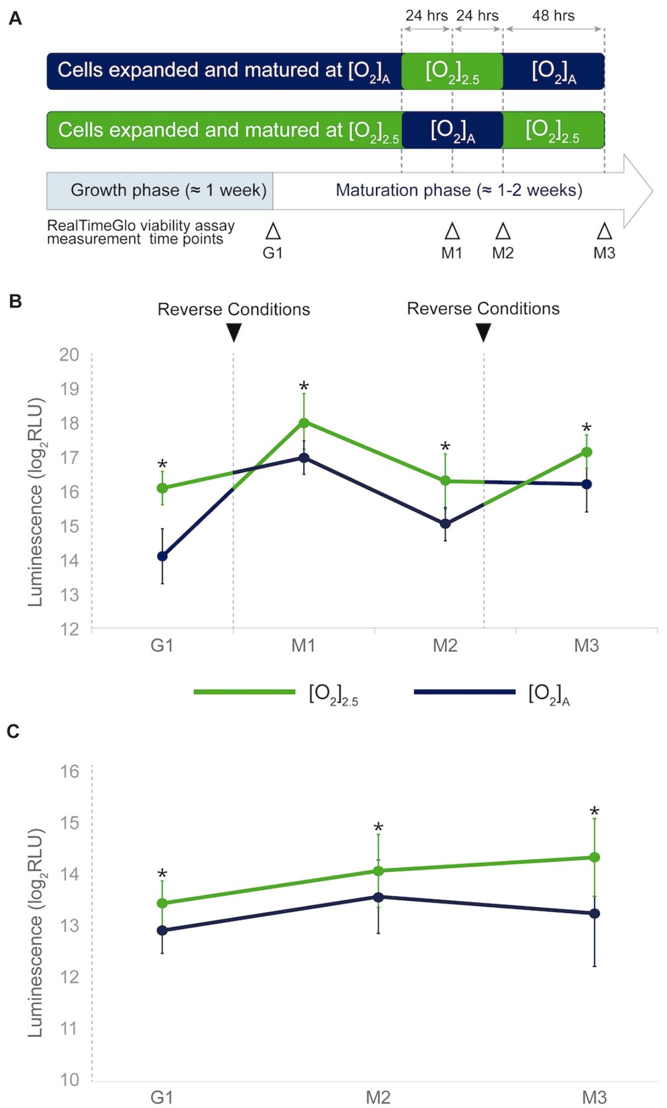

Figure 3. HCEnCs are adaptable to O_2 changes and can rapidly switch metabolic phenotypes. (A) In the experimental timeline for these experiments, HCEnCs were expanded and matured at $[O_2]_A$ and $[O_2]_{2.5}$ and exposed to periods of reversed $[O_2]$ conditions. Chemiluminescent signal intensity (RLU) from metabolically active cells was measured using RealTime-Glo Cell Viability Assay. Raw signal data were normalized with $\log_2$ transformation and means were compared using paired two-tailed Student's *t*-test (*$P < 0.05$). Data represent means ± SD, n = 5–7 corneas. (B) Data from experimental samples exposed to reversing $[O_2]$ conditions. (C) Data from control samples maintained under steady $[O_2]$ conditions.

OCR was measured with the sequential additions of oligomycin (to block H^+-ATPase), FCCP (to uncouple the mitochondrial inner membrane H^+ gradient), and rotenone and antimycin A (to block complexes I and III of the electron transport chain) (Fig. 4Ai). From the generated data, we calculated basal respiration, ATP-linked respiration, maximal respiration, spare capacity, and nonmitochondrial oxygen consumption (Fig. 4Bi). Experiments for each cornea were performed with a minimum of two technical replicates and at least five HCEnC cultures from different donors. We found that there were no differences in basal respiration or ATP-linked respiration between HCEnCs grown at $[O_2]_A$ and at $[O_2]_{2.5}$. However, significantly greater OCR values at $[O_2]_{2.5}$ than at $[O_2]_A$ were seen with proton leak (OCR in pmol/min/cell: $[O_2]_{2.5} = 0.0224 \pm 0.00735$; $[O_2]_A = 0.00448 \pm 0.00338$; $P = 0.002$) and nonmitochondrial oxygen consumption ($[O_2]_{2.5} = 0.134 \pm 0.0504$; $[O_2]_A = 0.00527 \pm 0.00506$; $P = 0.002$). A significant decrease was also noted with spare capacity ($[O_2]_{2.5} = 0.0134 \pm 0.0107$; $[O_2]_A = 0.103 \pm 0.0429$; $P = 0.015$).

Glycolysis was measured as ECAR after additions of oligomycin (mitochondrial ATP production is blocked and glycolysis is enhanced when the H^+-ATPase is blocked by oligomycin) and 2-DG (to block hexokinase in the glycolytic pathway; Fig. 4Aii). As anticipated at lower $[O_2]$ levels, basal glycolysis was significantly increased at $[O_2]_{2.5}$ (ECAR in mpH/min/cell: 0.0135 ± 0.00515) compared to that at $[O_2]_A$ (0.00578 ± 0.00158; $P = 0.019$), but the glycolytic reserve capacity was decreased (ECAR: $[O_2]_{2.5} = 0.00326 \pm 0.00124$; $[O_2]_A = 0.00620 \pm 0.00189$; $P = 0.015$; Fig. 4Bii).

Discussion

In vivo, HCEnCs are in an aqueous environment containing 2.8% O_2. However, nearly all studies on HCEnCs to date have used cultures under experimental conditions in room air (~18% O_2). In this study, we show that primary HCEnCs can successfully be cultured at $[O_2]_{2.5}$ and show considerable differences in cell metabolism including differences in reducing potential (viability assays), oxygen-consuming reactions, and glycolytic metabolism. Because primary HCEnCs are routinely used for experiments to address questions related to corneal endothelial function and dysfunction and are being investigated for use in cell-based therapeutics for corneal diseases, our data suggest that incorporating physiological O_2 levels in the culturing technique should be strongly considered.

Because of the closer approximation of $[O_2]_{2.5}$ to in vivo physiological $[O_2]$, we hypothesized that cells would demonstrate more favorable growth than in room air incubators.[18] Although their growth at $[O_2]_{2.5}$ was better, the difference was not significant. Although prior studies in bovine corneal endothelial cells have shown improved growth under 5% O_2 conditions,[30] our studies included corneal endothelial cells from

translational vision science & technology

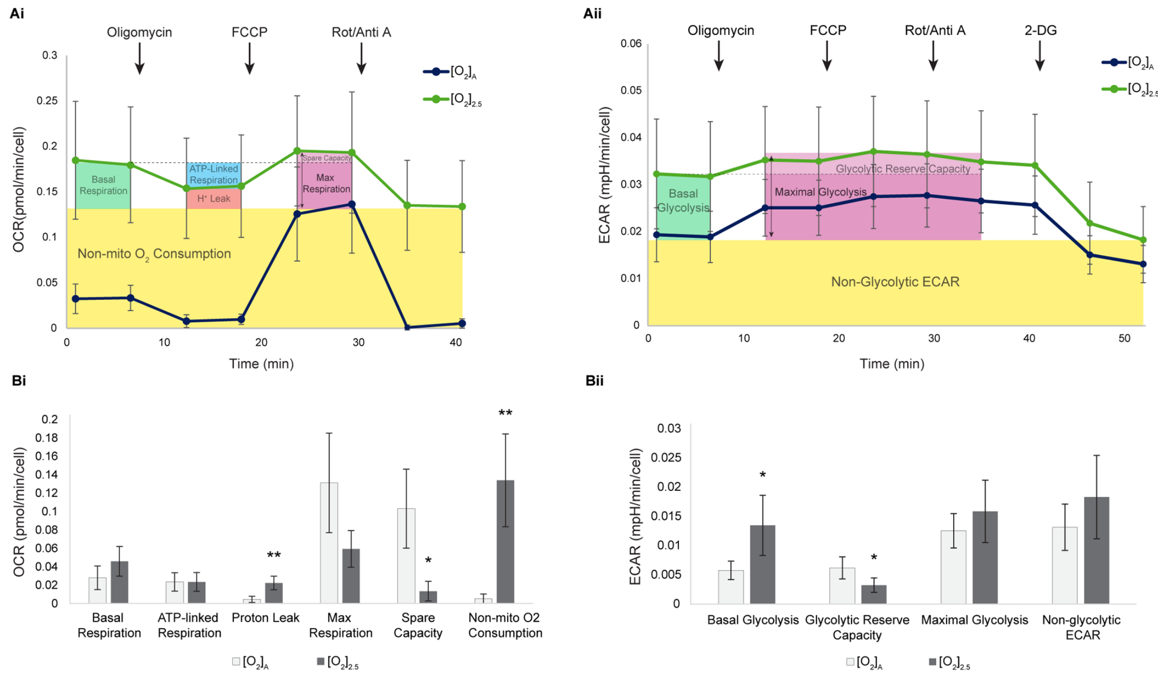

Figure 4. HCEnC grown at $[O_2]_A$ and $[O_2]_{2.5}$ have distinct metabolic phenotypes. Oxygen consumption rate (OCR) (Ai) and extracellular acidification rate (ECAR) (Aii) data plotted over time with drug additions as indicated. Colored boxes based on $[O_2]_{2.5}$ data illustrating the calculated values shown in panels Bi and Bii. $[O_2]_{2.5}$ (n = 6 corneas), $[O_2]_A$ (n = 5 corneas). (* $P < 0.05$, ** $P < 0.01$).

older humans, which may explain the discrepancy. For example, >50% of the cells in our study were senescent, which we attribute to the older age of the donors (mean age 81 years). The trend toward improved growth of primary FECD HCEnCs at $[O_2]_{2.5}$ versus that at $[O_2]_A$ suggests that FECD cells prefer the lower-O_2 environment for survival and cell proliferation. Oxidative stress is a central component to FECD pathophysiology, hypothesized to be perpetuated by the exposure of the cornea to UV light and a higher $[O_2]$ at the central corneal endothelium.[18,31,32] The physioxic $[O_2]$ levels of $[O_2]_{2.5}$ may provide an environment with reduced environmental oxidative stress compared to that at $[O_2]_A$, which is more favorable for cultured FECD cells and normal HCEnC cells. This suggests that the $[O_2]$ environment of standard room air cell culture incubators may confound findings from prior in vitro studies on the effects of oxidative stress on corneal endothelial cells.

We assayed CD44 expression in our cultures, as the $CD44^-$ subpopulation is targeted for corneal endothelial cell injection therapies.[3] $CD44^-$ cells are less likely to demonstrate endothelial-mesenchymal transition[33] and have an oxidative metabolic phenotype.[25,34] We wanted to know if the $[O_2]$ can alter CD44 expression and thus the cellular phenotype. Although we did not find a consistent up- or downregulation of CD44 according to the culture $[O_2]$ environment, our cells did significantly differ in their oxidative and glycolytic metabolic phenotypes, suggesting that CD44 may not be an independent phenotype marker. This is not surprising, because CD44 expression has also been noted to vary in different cell types in response to cellular senescence, oxidative damage, and epigenetic changes, which may also account for the variable CD44 expression seen in our cultures.[9,34,35]

The metabolic phenotype of corneal endothelial cells may be intimately linked to their function of ion transport and may play a central role in disease phenotype. Oxidative respiration via glutamine catabolism supports the maintenance of corneal hydration via the ion transporter SLC4A11 (Solute Carrier Family Member 11), and energy deficiency is postulated to play a role in the pathophysiology of SLC4A11-associated endothelial diseases, such as congenital hereditary endothelial dystrophy and FECD.[36,37] We therefore performed an overview of metabolic function of HCEnCs under both $[O_2]$ conditions to assess their oxygen use and dependence on glycolysis. We found that under both conditions, cells had similar OCRs for basal respiration, suggesting that the lower $[O_2]$ condition was not limiting for metabolism. Likewise, ATP-linked respiration was also maintained under both

translational vision science & technology

conditions, suggesting that ATP is also not limited. However, baseline glycolysis was increased in HCEnCs grown at $[O_2]_{2.5}$ than in cells grown at $[O_2]_A$, with a concurrent decrease in glycolytic reserve capacity. Although we do not know the mechanism underlying the increase in glycolysis at $[O_2]_{2.5}$, it is not an unexpected finding. The corneal endothelium has strong glycolytic and oxidative metabolic capacities and can rapidly increase glycolysis under anerobic conditions to meet the energy needs of the cells to maintain corneal hydration.[38] We observed the ability of HCEnC to rapidly adapt to their $[O_2]$ environment in our viability assay and suspect a similar mechanism is involved. $[O_2]$ conditions in the anterior chamber vary in diseases of the corneal endothelium (FECD and bullous keratopathy) but also with the common condition of pseudophakia.[18,39] The rapid adaptability we observed for endothelial metabolism under $[O_2]_A$ and $[O_2]_{2.5}$ may serve to meet the energy needs of the corneal endothelium under these different $[O_2]$. However, because corneal endothelial cell metabolism is associated with ion transport function, the long-term effects on overall function and survival are not known and could impact our approach towards endothelial diseases (e.g., the timing of cataract surgery in endothelial disease) and $[O_2]$ culture conditions for cell transplantation.

Another significant difference observed between HCEnC culture conditions was a lower spare capacity at $[O_2]_{2.5}$ than at $[O_2]_A$. The spare respiratory capacity represents the flexibility of the cell to increase oxidative metabolism to meet an increased energy demand. The value is dependent on suitable substrate availability and the health of the mitochondrial electron transport chain.[40] Although decreased spare capacity is frequently attributed to the latter (mitochondrial dysfunction), our observed trends of improved cell growth at $[O_2]_{2.5}$ versus that at $[O_2]_A$ for both FECD and normal HCEnCs would be unlikely in the setting of mitochondrial dysfunction. We suspect that differences in substrate use account for the decrease in spare respiratory capacity, because substrate-specific changes in spare capacity in corneal endothelial cells have been described.[41] In our data, at $[O_2]_{2.5}$, there was an increase in basal glycolysis, with lactate generated from pyruvate, as suggested by an increased ECAR. This would limit the amount of pyruvate available for the tricarboxylic acid cycle and thus downstream oxidative metabolism, thereby potentially limiting the substrate availability for spare respiratory capacity. This mechanism for reduced spare respiratory capacity has been demonstrated under hypoxic conditions and with variations in substrate availability in cardiac myocytes.[42]

Variation in substrate utilization under different culture conditions for HCEnCs is also supported by our observation of increased proton leak at $[O_2]_{2.5}$. Increased proton leak can be associated with increased SLC4A11 activity which may reflect a preference for glutamine metabolism at physiologic $[O_2]$. Proton leak reflects dissipation of the proton gradient created by the electron transport chain across the inner mitochondrial membrane.[43] Reducing the proton gradient also decreases the formation of reactive oxygen species by the electron transport chain. SLC4A11, which is a H^+-transporting channel whose activity is increased in the presence of glutamine catabolism, can regulate proton leak in mitochondria of corneal endothelial cells.[44] This underscores the importance of matching metabolic substrates to the $[O_2]$ condition for cell growth and function.

Another prominent finding in our metabolic assays was the significant increase in nonmitochondrial oxygen consumption at $[O_2]_{2.5}$ compared to that at $[O_2]_A$. Nonmitochondrial oxygen consumption may reflect increased activity of NADPH oxidases (NOX) to produce reactive oxygen species with both protective and pathologic functions.[45–47] Increased NADPH production as a byproduct of glycolysis has been hypothesized to favor NOX activity.[46] Similarly, the increased basal glycolysis in our cells at $[O_2]_{2.5}$ may have favored NOX activity and thus explains the observed increase in nonmitochondrial oxygen consumption. Nonmitochondrial oxygen consumption can serve to maintain reactive oxygen species signaling, which is paramount in corneal endothelium. Indeed, antioxidant drugs such as N-acetylcysteine and sulforaphane represent one strategy investigated for treating corneal endothelial diseases.[32,48–50]

Our study data must be interpreted with two particular points in mind. First, the corneas used in these experiments were mostly from older donors (mean age ~70 years). Although this provides an excellent comparison for studies of corneal diseases associated with aging such as FECD, it may not be comparable to other studies using HCEnC cultures from young donors. The second point to consider when interpreting these findings is the $[O_2]$ environment for the assay procedures. Whereas cells were grown and matured long term in their respective environments, viability and metabolic assays were performed under room air. Thus acute O_2 stress may have been a factor. Nevertheless, the chronic adaptive changes occurring at both $[O_2]$ conditions are readily apparent in our data.

The culture of cells under conditions that most closely resemble their normal physiological environment has many benefits. These include maintaining the native phenotype and function and reducing external stressors. The results of this descriptive analysis are an initial step toward identifying and optimizing culture conditions for in vitro mechanistic studies and emerging cell replacement therapies.

Acknowledgments

The authors thank Bruce Troen, Kenneth Seldeen, and Ramkumar Thiyagarajan for their assistance with the metabolism studies, and Jack M. Sullivan and Michael Fautsch for critical review of the manuscript.

Supported by the National Eye Institute (NEI) and the Office of Research on Women's Health (ORWH) NIH K08 EY029007 (S.P.P.); the Jacobs School of Medicine and Biomedical Sciences, State University of New York at Buffalo, Summer Research Fellowship (N.P., C.M., J.C.F.); and facilities and resources provided by the VA Western New York Healthcare System. The contents of this work do not represent the views of the Department of Veterans Affairs or the United States government.

Disclosure: **S.P. Patel,** None; **B.C. Gonzalez,** None; **N. Paone,** None; **C. Mueller,** None; **J.C. Floss,** None; **M.E. Sousa,** None; **M.Y. Shi,** None

References

1. Eye Bank Association of America. 2019 Eye Banking Statistical Report. *2019 Eye Banking Statistical Report*. 2020; Washington, DC: Eye Bank Association of America.
2. Van Meter WS. Analysis of Surgical Use and Indications for Corneal Transplant. *2019 Eye Banking Statistical Report*. 2020; Washington, DC: Eye Bank Association of America.
3. Kinoshita S, Koizumi N, Ueno M, et al. Injection of cultured cells with a ROCK inhibitor for bullous keratopathy. *N Engl J Med*. 2018;378:995–1003.
4. Ong HS, Ang M, Mehta J. Evolution of therapies for the corneal endothelium: past, present and future approaches. *Br J Ophthalmol*. 2021;105:454–467.
5. Numa K, Imai K, Ueno M, et al. Five-year follow-up of first 11 patients undergoing injection of cultured corneal endothelial cells for corneal endothelial failure. *Ophthalmology*. 2021;128:504–514.
6. Jalimarada SS, Ogando DG, Bonanno JA. Loss of ion transporters and increased unfolded protein response in Fuchs' dystrophy. *Mol Vis*. 2014;20:1668–1679.
7. Joyce NC. Proliferative capacity of corneal endothelial cells. *Exp Eye Res*. 2012;95:16–23.
8. Joyce NC, Harris DL, Zhu CC. Age-related gene response of human corneal endothelium to oxidative stress and DNA damage. *Invest Ophthalmol Vis Sci*. 2011;52:1641–1649.
9. Joyce NC, Zhu CC, Harris DL. Relationship among oxidative stress, DNA damage, and proliferative capacity in human corneal endothelium. *Invest Ophthalmol Vis Sci*. 2009;50:2116–2122.
10. Matthaei M, Zhu AY, Kallay L, Eberhart CG, Cursiefen C, Jun AS. Transcript profile of cellular senescence-related genes in Fuchs endothelial corneal dystrophy. *Exp Eye Res*. 2014;129:13–17.
11. Zhu C, Joyce NC. Proliferative response of corneal endothelial cells from young and older donors. *Invest Ophthalmol Vis Sci*. 2004;45:1743–1751.
12. Zhu C, Rawe I, Joyce NC. Differential protein expression in human corneal endothelial cells cultured from young and older donors. *Mol Vis*. 2008;14:1805–1814.
13. Carreau A, El Hafny-Rahbi B, Matejuk A, Grillon C, Kieda C. Why is the partial oxygen pressure of human tissues a crucial parameter? Small molecules and hypoxia. *J Cell Mol Med*. 2011;15:1239–1253.
14. Braunschweig L, Meyer AK, Wagenfuhr L, Storch A. Oxygen regulates proliferation of neural stem cells through Wnt/beta-catenin signalling. *Mol Cell Neurosci*. 2015;67:84–92.
15. Chen C, Tang Q, Zhang Y, Yu M, Jing W, Tian W. Physioxia: a more effective approach for culturing human adipose-derived stem cells for cell transplantation. *Stem Cell Res Ther*. 2018;9:148.
16. Shin DY, Huang X, Gil CH, Aljoufi A, Ropa J, Broxmeyer HE. Physioxia enhances T-cell development ex vivo from human hematopoietic stem and progenitor cells. *Stem Cells*. 2020;38:1454–1466.
17. Stuart JA, Fonseca J, Moradi F, et al. How supraphysiological oxygen levels in standard cell culture affect oxygen-consuming reactions. *Oxid Med Cell Longev*. 2018;2018:8238459.
18. Huang AJ, Shui YB, Han YP, Bai F, Siegfried CJ, Beebe DC. Impact of corneal endothelial dysfunctions on intraocular oxygen levels in human eyes. *Invest Ophthalmol Vis Sci*. 2015;56:6483–6488.
19. Maly IV, Hofmann WA. Effect of palmitic acid on exosome-mediated secretion and invasive motility in prostate cancer cells. *Molecules*. 2020;25:2722.

20. Singh JS, Haroldson TA, Patel SP. Characteristics of the low density corneal endothelial monolayer. *Exp Eye Res*. 2013;115:239–245.
21. Downie LE, Choi J, Lim JK, Chinnery HR. Longitudinal changes to tight junction expression and endothelial cell integrity in a mouse model of sterile corneal inflammation. *Invest Ophthalmol Vis Sci*. 2016;57:3477–3484.
22. Langford MP, Gosslee JM, Liang C, Chen D, Redens TB, Welbourne TC. Apical localization of glutamate in GLAST-1, glutamine synthetase positive ciliary body nonpigmented epithelial cells. *Clin Ophthalmol*. 2007;1:43–53.
23. Laursen AB. Concentrations of some metabolites in the aqueous humour of human senile cataractous eyes. *Acta Ophthalmol (Copenh)*. 1975;53:369–377.
24. Laursen AB, Lorentzen SE. Glucose, pyruvate and citrate concentrations in the aqueous humour of human cataractous eyes. *Acta Ophthalmol (Copenh)*. 1974;52:477–489.
25. Hamuro J, Ueno M, Asada K, et al. Metabolic plasticity in cell state homeostasis and differentiation of cultured human corneal endothelial cells. *Invest Ophthalmol Vis Sci*. 2016;57:4452–4463.
26. Munoz-Sanchez J, ME Chanez-Cardenas. The use of cobalt chloride as a chemical hypoxia model. *J Appl Toxicol*. 2019;39:556–570.
27. Talks KL, Turley H, Gatter KC, et al. The expression and distribution of the hypoxia-inducible factors HIF-1alpha and HIF-2alpha in normal human tissues, cancers, and tumor-associated macrophages. *Am J Pathol*. 2000;157:411–421.
28. Handy DE, Loscalzo J. Redox regulation of mitochondrial function. *Antioxid Redox Signal*. 2012;16:1323–1367.
29. Rolfe DF, Brand MD. The physiological significance of mitochondrial proton leak in animal cells and tissues. *Biosci Rep*. 1997;17:9–16.
30. Zagorski Z, Gossler B, Naumann GO. Effect of low oxygen tension on the growth of bovine corneal endothelial cells in vitro. *Ophthalmic Res*. 1989;21:440–442.
31. Jurkunas UV, Bitar MS, Funaki T, Azizi B. Evidence of oxidative stress in the pathogenesis of Fuchs endothelial corneal dystrophy. *Am J Pathol*. 2010;177:2278–2289.
32. Liu C, Miyajima T, Melangath G, et al. Ultraviolet A light induces DNA damage and estrogen-DNA adducts in Fuchs endothelial corneal dystrophy causing females to be more affected. *Proc Natl Acad Sci USA*. 2020;117:573–583.
33. Hamuro J, Toda M, Asada K, et al. Cell homogeneity indispensable for regenerative medicine by cultured human corneal endothelial cells. *Invest Ophthalmol Vis Sci*. 2016;57:4749–4761.
34. Hamuro J, Numa K, Fujita T, et al. Metabolites interrogation in cell fate decision of cultured human corneal endothelial cells. *Invest Ophthalmol Vis Sci*. 2020;61:10.
35. Lowe D, Raj K. Premature aging induced by radiation exhibits pro-atherosclerotic effects mediated by epigenetic activation of CD44 expression. *Aging Cell*. 2014;13:900–910.
36. Zhang W, Frausto R, Chung DD, et al. Energy shortage in human and mouse models of SLC4A11-associated corneal endothelial dystrophies. *Invest Ophthalmol Vis Sci*. 2020;61:39.
37. Zhang W, Li H, Ogando DG, et al. Glutaminolysis is essential for energy production and ion transport in human corneal endothelium. *EBioMedicine*. 2017;16:292–301.
38. Riley MV, Winkler BS. Strong Pasteur effect in rabbit corneal endothelium preserves fluid transport under anaerobic conditions. *J Physiol*. 1990;426:81–93.
39. Siegfried CJ, Shui YB, Holekamp NM, Bai F, Beebe DC. Oxygen distribution in the human eye: relevance to the etiology of open-angle glaucoma after vitrectomy. *Invest Ophthalmol Vis Sci*. 2010;51:5731–5738.
40. Marchetti P, Fovez Q, Germain N, Khamari R, Kluza J. Mitochondrial spare respiratory capacity: mechanisms, regulation, and significance in non-transformed and cancer cells. *FASEB J*. 2020;34:13106–13124.
41. Ogando DG, Bonanno JA. RNA sequencing uncovers alterations in corneal endothelial metabolism, pump and barrier functions of Slc4a11 KO mice. *Exp Eye Res*. 2022;214:108884.
42. Pfleger J, He M, Abdellatif M. Mitochondrial complex II is a source of the reserve respiratory capacity that is regulated by metabolic sensors and promotes cell survival. *Cell Death Dis*. 2015;6:e1835.
43. Cadenas S. Mitochondrial uncoupling, ROS generation and cardioprotection. *Biochim Biophys Acta Bioenerg*. 2018;1859:940–950.
44. Ogando DG, Choi M, Shyam R, Li S, Bonanno JA. Ammonia sensitive SLC4A11 mitochondrial uncoupling reduces glutamine induced oxidative stress. *Redox Biol*. 2019;26:101260.
45. Ago T, Kuroda J, Pain J, Fu C, Li H, Sadoshima J. Upregulation of Nox4 by hypertrophic stimuli promotes apoptosis and mitochondrial

dysfunction in cardiac myocytes. *Circ Res*. 2010;106:1253–1264.

46. Baillet A, Hograindleur MA, El Benna J, et al. Unexpected function of the phagocyte NADPH oxidase in supporting hyperglycolysis in stimulated neutrophils: key role of 6-phosphofructo-2-kinase. *FASEB J*. 2017;31:663–673.
47. Lu W, Hu Y, Chen G, et al. Novel role of NOX in supporting aerobic glycolysis in cancer cells with mitochondrial dysfunction and as a potential target for cancer therapy. *PLoS Biol*. 2012;10:e1001326.
48. Katikireddy KR, White TL, Miyajima T, et al. NQO1 downregulation potentiates menadione-induced endothelial-mesenchymal transition during rosette formation in Fuchs endothelial corneal dystrophy. *Free Radic Biol Med*. 2018;116:19–30.
49. Kim EC, Toyono T, Berlinicke CA, et al. Screening and characterization of drugs that protect corneal endothelial cells against unfolded protein response and oxidative stress. *Invest Ophthalmol Vis Sci*. 2017;58:892–900.
50. Ziaei A, Schmedt T, Chen Y, Jurkunas UV. Sulforaphane decreases endothelial cell apoptosis in Fuchs endothelial corneal dystrophy: a novel treatment. *Invest Ophthalmol Vis Sci*. 2013;54:6724–6734.
51. Repp DJ, Hodge DO, Baratz KH, McLaren JW, Patel SV. Fuchs' endothelial corneal dystrophy: subjective grading versus objective grading based on the central-to-peripheral thickness ratio. *Ophthalmology*. 2013;120:687–694.